J Mater Sci (2007) 42:2463–2470
DOI 10.1007/s10853-006-1295-x

High strain rate behavior of 4-step 3D braided composites under compressive failure

Baozhong Sun · Bohong Gu

Received: 27 June 2005 / Accepted: 30 January 2006 / Published online: 23 December 2006

Abstract The out-of-plane and in-plane compressive failure behavior of 4-step 3D braided composite materials was investigated at quasi-static and high strain rates. The out-of-plane and in-plane direction compressive tests at high strain rates from 800/s to 3,500/s were tested with the split Hopkinson pressure bar (SHPB) technique. The quasi-static compressive tests were conducted on a MTS 810.23 tester and compared with those at high strain rates. The comparisons indicate that the failure stress, failure strain and compressive stiffness both for out-of-plane and in-plane loading directions are rate sensitive. For example, the failure stress, failure strain and stiffness are 55.19 MPa, 6.70% and 1.35 GPa respectively as opposed to 145.00 MPa, 1.21% and 13.50 GPa respectively for strain rate of 2,500 s^{-1} under in-plane compression. The 3D braided composites have higher values of failure stress and strain for out-of-plane than for in-plane compression at the same strain rate; however, the in-plane compression stiffness is higher than that of out-of-plane compression at high strain rates. The compressive failure mode of 3D braided composites in the out-of-plane direction is mainly shear failure at various strain rates, while for the in-plane direction it is mainly cracking of matrix.

B. Sun · B. Gu (✉)
College of Textiles, Donghua University, Shanghai 200051, China
e-mail: gubh@dhu.edu.cn

B. Gu
Department of Textile Engineering, Zhongyuan Institute of Technology, Zhengzhou, Henan Province 450007, China

Introduction

The response of 3D textile composites under impulsive loading is of interest in a variety of applications, such as ballistic impact protection. Understanding and characterizing the response of the 3D textile composites at high strain rates is necessary for structural design and analysis for impulsive loading because the mechanical properties at high strain rates are the basic parameters for design. Strain rate effects on unidirectional and laminated composites have been studied experimentally by many researchers. Hosur et al. [1] tested the compressive properties of carbon/epoxy laminated composites at strain rates of 82, 164 and 817 s^{-1}. The results indicated that the dynamic strength and stiffness exhibited considerable increase as compared with quasi-static. Haque et al. [2] investigated the compressive stress–strain responses of S2-glass–vinyl ester woven fabric composites in the through-thickness direction as well as the through-filler direction at strain rates from 490–1,470 s^{-1} and temperatures from 23 °C to 204 °C. The results showed that moisture and temperature degrade the compressive failure strength under high strain rate loading. The failure strength and failure strain of both dry and wet samples seemed to increase under high strain rate loading. Hosur et al. [3] conducted compressive tests on 37 layer satin weave carbon/epoxy laminates at different in-plane directions and strain rates. There was a considerable increase in stiffness at high strain rate loading as compared to static loading. Ultimate strength and strain of the woven carbon/epoxy composites varied considerably with the orientation of the fibers to loading direction.

Strain-rate effects on 3D textile structural composites have rarely been studied. Hosur et al. [4] studied

the compressive behavior of 2D-Plain, 3D-Pin reinforced, and 3D-Stitched woven fabric composites at strain rates of 327, 436 and 544 s^{-1}. Hosur et al. [5] also investigated stitched and unstitched woven carbon/epoxy laminates under high strain rate compression loading. The effects of an unstitched/stitched configuration, fabric type and loading directions on compressive properties were discussed. Sun et al. [6] studied the compressive properties of 3D angle-interlock E-glass/vinyl ester woven composites under high strain rates. The stress–strain curves of the 3D woven fabric composites under compression were strain rate sensitive. The compressive stiffness and maximum compressive stress increased linearly with the increase of strain rate. Sun et al. [7] also studied in-plane and out-of-plane mechanical properties of two types of 4-step 3-dimensional braided composite, 8×4 and 8×6 arrays in rectangular cross-section, at various strain rates. The results showed that the mechanical behavior of the materials is strain rate sensitive and the compressive stiffness increases with increasing strain rate. The failure compressive stress, failure strain and failure mode were discussed. However, the braided composite specimen were not compressed to failure as the 3D woven composites in the reference [6] because the low velocity of strike bar and intensity of the incident wave generated by the impact of the 200 mm striker bar on the 600 mm incident bar. The incident wave was mostly reflected and only a small part transmitted through the specimen. The transmission wave could not make specimens compressive damaged and this can be proved by the post-mortem photographs [7].

In this study, a 300 mm striker bar was used and the velocity of strike bar was adjusted to cause compressive failure of the 3D braided composites. The in-plane and out-of-plane compressive properties of 4-step 3D braided composites under quasi-static and high strain rate had been tested on a MTS 810.23 tester and split Hopkinson pressure bar (SHPB) respectively. The in-plane and out-of-plane compressive stress–strain curves, compressive stiffness, failure stress and strain at quasi-static and high-strain-rate testing were compared. The failure modes of 3D braided composites at various strain rates are also discussed.

Experimental

Materials and fabrication of specimen

The 3D E-glass braided composites were fabricated from 3D E-glass braided preform with rectangular cross-sections of 8×6 arrays by a 4-step 1×1 method and vinyl ester resin in the RTM process. The void content in the 3D braided composite was less than 1.0% and fiber volume fraction approximated to be 50%. All the specimens had the same length of 8.5 mm and cross-section of 5.6×8.5 mm. Compression tests were conducted both in the out-of-plane and in-plane directions, as shown in Fig. 1.

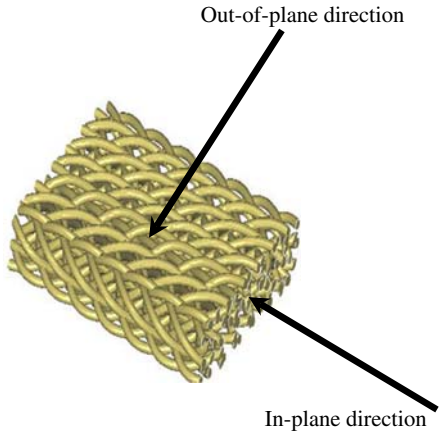

Fig. 1 Schematic of compression direction of 3D braided composite

As the introduction by Chou [8], the 4-step braiding process requires four distinct Cartesian motions of the yarns in the fabric cross-section plane in each machine cycle. The 4-step braiding process is shown in Fig. 2 for a 1×1 set-up in which the yarn carriers are arranged in a rectangular plane with 12 columns and 4 layers. The yarn carries are indicated by the circles, and can move along the horizontal and vertical direction tracks. The process is termed 1×1 if the distance traveled by a carrier in each machine step is equal to the inter-yarn spacing in the horizontal or vertical direction. The braiding angle is the most important parameter except mechanical properties of braided tow that influence the stiffness and strength of braided composites. The braiding angle is the angle between the braided yarn in the braided preform surface and the longitudinal axis of braided preform.

Quasi-static and high-strain-rate compression testing

To determine the static compressive properties of 3D braided composites, quasi-static compression tests were conducted on a MTS 810.23 servo-hydraulic materials tester with a constant crosshead speed of 1 mm/min. The strain rate corresponding to the speed approximates to 10^{-3} s^{-1}. At least three composite coupons were tested and the average compression stress vs. strain curve was obtained.

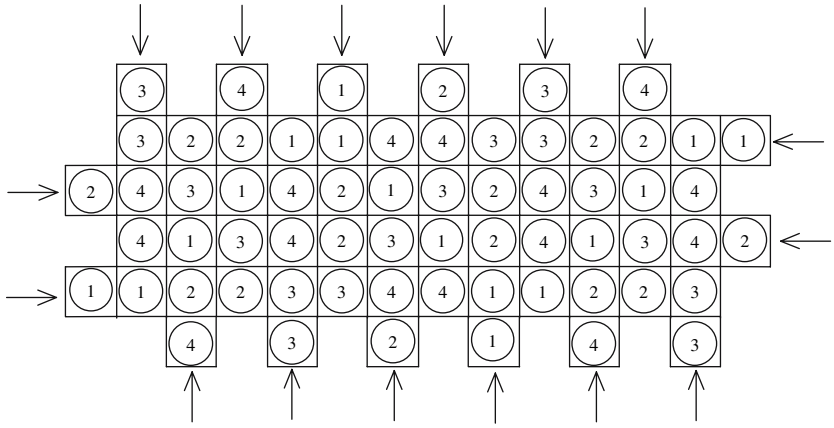

Fig. 2 Cross-section and yarn carrier configuration in a 4-step 1 × 1 braiding

The high-strain-rate compression tests, at rates ranging from of 800 to 3,500 s^{-1}, were performed on a modified SHPB [9]. The SHPB technique has been widely used in high-strain-rate testing of materials. Detailed information on the principles of SHPB apparatus could be found in elsewhere [6, 7, 9]. In order to obtain the mechanical properties of 3D braided composites which fail in compression at high strain rates, there are two methods: the one is to increase the strike velocity of strike bar at the cost of lower ranges of strain rate; another is to use a longer strike bar, which does not decrease the range of strain rate. The second method is used for high strain rate compression test hereinafter. The specimens were photographed after test to illustrate the damage mode of 3D braided composite under high strain rate compression.

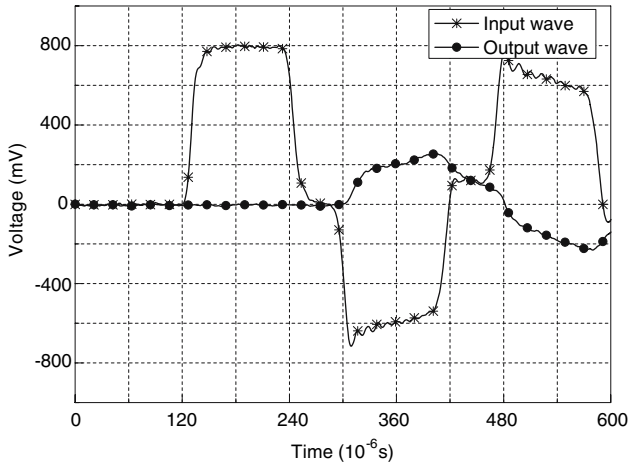

Fig. 3 Typical signals for 3D braided composites in the out-of-plane compression

Results and discussions

Strain rate data

The typical strain waves from out-of-plane and in-plane compression, which were detected by the strain-gages mounted on the incident and transmission bars, are presented in Figs. 3 and 4 respectively. It could be shown that the shape of the transmission wave from out-of-plane compression is different from that of in-plane compression.

Assuming the modulus, cross-sectional area and density of the incident and transmission bar in SHPB apparatus are denoted by E_b, A_b and ρ_b and those of the specimen are E_s, A_s and ρ_s, the equations for the strain-rate strain ($\dot{\varepsilon}$), and stress (σ) of the specimen are given by [9]:

$$\dot{\varepsilon}(t) = -\frac{2C_0}{L_s}\varepsilon_R(t) \quad (1)$$

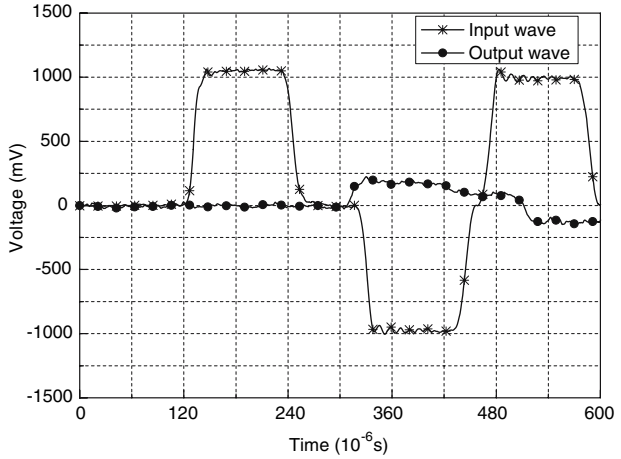

Fig. 4 Typical signals for 3D braided composites in the in-plane compression

$$\varepsilon(t) = -\frac{2C_0}{L_s}\int_0^t \varepsilon_R(t)\mathrm{d}t \tag{2}$$

$$\sigma(t) = \frac{E_b A_b}{A_s}\varepsilon_T(t) \tag{3}$$

where $C_0 = \sqrt{E_b/\rho_b}$ is the longitudinal wave velocity in the bar, L_s is the specimen length, and ε_R (t) and ε_T (t) are the strain gage signal of the reflected and the transmitted pulses respectively. Equations (1) through (3) are based on the assumption that the dynamic forces on both sides of the specimen are equal and can be expressed as:

$$\varepsilon_I + \varepsilon_R = \varepsilon_T \tag{4}$$

Equations (1)–(3) give the average stress and strain in the specimen as a function of time. The equations also show that the strain can be obtained by integrating the reflected pulse and the stress in the specimen from the transmitted pulse.

From Eq. (3), the stress is a function of the amplitude of the transmission wave, i.e., the stresses have same shape as the corresponding transmission wave. According to the input and output waves, the stress–strain curves could be calculated with Eqs. (1)–(3) at each strain rate. The stress vs. strain curves of 3D braided composites compressed at various strain rates in the out-of-plane and in-plane direction are shown in Figs. 5 and 6 respectively. Figure 5 indicates that the stresses vs. strain curves are rate sensitive and have bilinear features. The initial linear elastic response is followed by another smaller slope linear elastic response at each of the strain rates including quasi-static and high strain rate loading. Furthermore, the compressive stiffness and peak stress increases with increasing of strain rate and the failure strain is decreased with increasing strain rate. Figure 6 depicts that the stress linear-increases initially and then decreases gradually after the stress reaches a maximum value. It is clear that the stress–strain curves under the in-plane compressive testing of 3D braided composites are also strain rate sensitive. However, it can be observed that the shape of stress–strain curves in Figs. 5 and 6 are completely different. Plastic deformation behavior occurs after elastic deformation in the out-of-plane compression of 3D braided composites, while only linear elastic behavior from zero to peak stress occurs in the case of in-plane compression. From Figs. 5 and 6, the compressive stiffness, peak compression stress and failure strain in two material directions have been obtained and listed in Tables 1. In order to understand mechanical behavior of 3D braided composites, the compressive stiffness, and peak stress and failure strain were discussed in detail as follows.

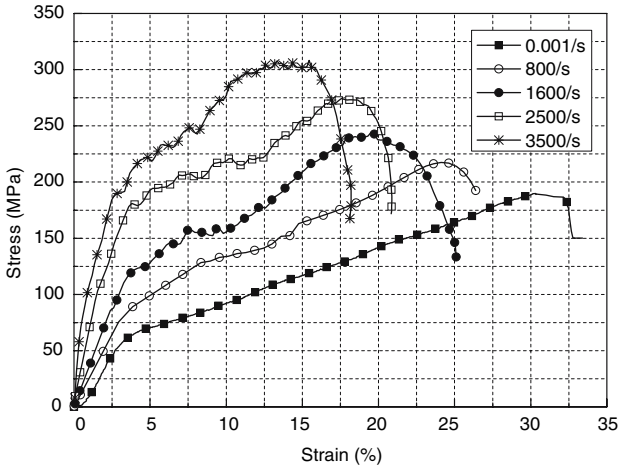

Fig. 5 Stress–strain curves of the 3D braided composites at various strain rates in the out-of-plane direction

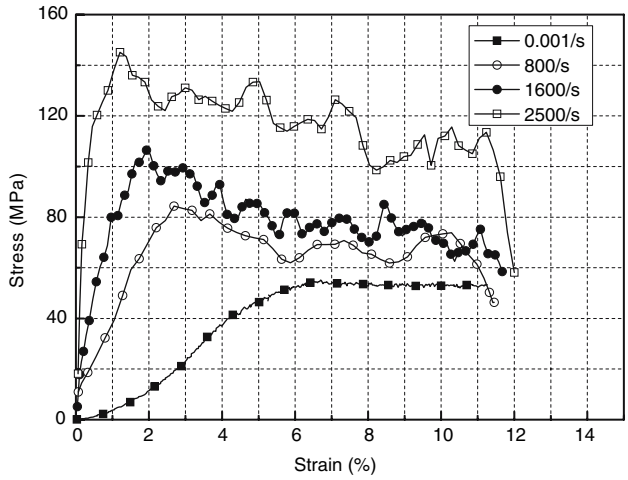

Fig. 6 Stress–strain curves of the 3D braided composites at various strain rates in the in-plane direction

Table 1 Mechanical properties of the 3D braided composites at various strain rates in the out-of-plane direction

Strain rate (s^{-1})	Stiffness (GPa)	Peak stress (MPa)	Failure strain (%)
0.001	1.89	189.88	30.30
800	2.53	217.41	23.12
1,600	3.78	242.66	19.51
2,500	6.70	274.08	17.45
3,500	12.30	308.16	16.13

Compression stiffness in out-of-plane direction and in-plane direction

Figure 7 depicts the compression stiffness of 3D braided composites in two material directions at various strain rates. It can be shown that the compression stiffness non-linearly increases the strain rate both in the in-plane and out-of-plane direction. In quasi-static loading, the compressive stiffness of 3D braided composites in the out-of-plane direction is larger than that in the in-plane direction (Table 2). But in high-strain-rate loading, the compressive stiffness in the in-plane direction is larger than that of the out-of-plane direction at same strain rate. The reason why the stiffness is higher for out-of-plane compression than that of in-plane compression in quasi-static is that the stress in the composites has sufficient time to reach equilibrium between braided tows and matrix, and then the matrix dominates the stress transfer. The braided composite at quasi-static condition is similar with transverse isotropic materials to some extent (see Fig. 1). Additionally the braided tows are in crimp form at in-plane direction, and contribute a lower modulus compared with the unidirectional lamina. These lead to the low stiffness under compression at in-plane direction. At high strain rate compression, the stress wave mostly transfers from braided tows because of higher Young's modulus of glass fibers than epoxy matrix. Then the stiffness of the composite in-plane compression is determined by the braided tows while at out-of-plane compression by matrix. This induces the higher compression stiffness at in-plane direction in high strain rate compression.

Furthermore, the compressive stiffness changes more rapidly in the in-plane direction than in the out-of-plane direction. This shows that the compressive stiffness is more sensitive to strain rate in the case of in-plane loading than that in the case of out-of-plane loading.

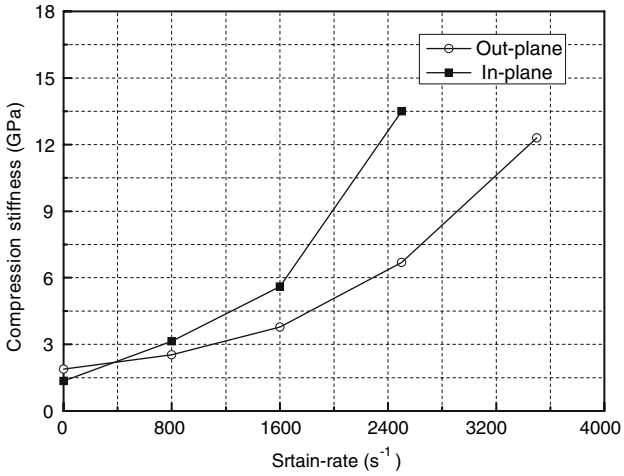

Fig. 7 Compressive stiffness of 3D braided composites in the out-of-plane and in-plane directions at various strain rates

Table 2 Mechanical properties of the 3D braided composites at various strain rates in the in-plane direction

Strain rate (s^{-1})	Stiffness (GPa)	Peak stress (MPa)	Failure strain (%)
0.001	1.35	55.19	6.70
800	3.14	82.21	2.93
1,600	5.60	105.00	1.93
2,500	13.50	145.00	1.21

Peak stress in two compression directions

Figure 8 depicts the peak compression stress of 3D braided composites at various strain rates in two compression directions. From Fig. 8, the peak stresses both for out-of-plane and in-plane compression increase with increasing strain rate. It was found that two curves are nearly parallel. However, the out-of-plane peak stress is higher than the in-plane peak stress at same strain rate. The relationships are as follows:

$$\sigma_{\max} = 189.79 + 0.034\dot{\varepsilon} \quad \text{(out - of - plane)} \tag{5}$$

$$\sigma_{\max} = 54.00 + 0.035\dot{\varepsilon} \quad \text{(in - plane)} \tag{6}$$

In Eqs. (5) and (6), the coefficients of $\dot{\varepsilon}$ are nearly equal. This shows that the failure stresses of the materials exhibit nearly same sensitive to strain rate.

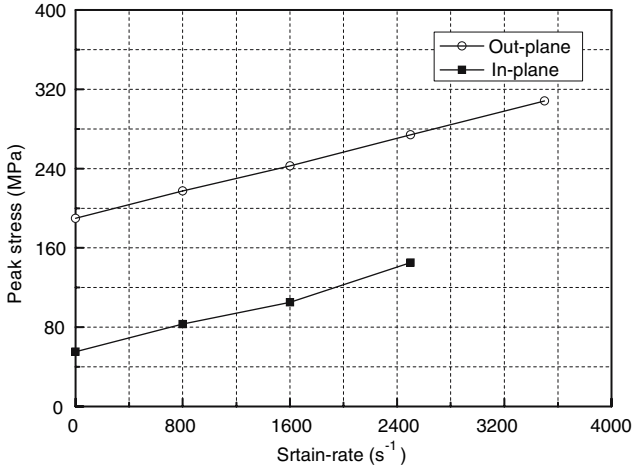

Fig. 8 Peak stress of 3D braided composites in the out-of-plane and in-plane directions at various strain rates

Compressive failure strain in two directions

The failure strain of the 3D braided composites in two compression directions at various strain rates is shown in Fig. 9. It was found that the out-of-plane failure strain non-linearly decreases with increasing strain rate. Furthermore, the out-of-plane failure strains at higher strain rates are drastically decreased compared with quasi-static out-of-plane compression. The in-plane failure strain also shows the same trend with out-of-plane failure strain. It can also be concluded that the failure strains for both out-of-plane and in-plane are rate sensitive. From Fig. 9, the 3D braided composites have larger failure strain for the out-of-plane direction than in the in-plane direction.

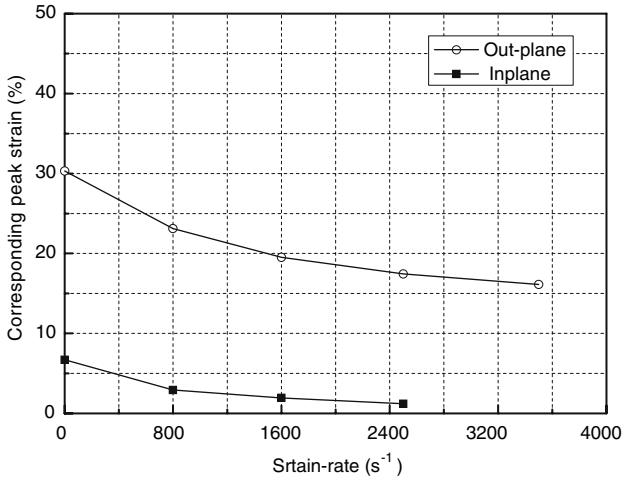

Fig. 9 Compressive failure strain of 3D braided composites in the out-of-plane and in-plane directions at various strain rates

Failure modes of the 3D braided composites under high strain rate compression in two directions

The photographs in Fig. 10(a) illustrate the damage of 3D braided composites at various strain rates under out-of-plane loading. It is observed that shear deformation occurs at various strain rates and the main failure mode is shear failure. With increasing strain rate, the composites are compressed almost into debris as shown in Fig. 10(a). Figure 11 shows the local damage of composite coupons at different strain rates. Figure 11 (a) and (b) show the large crack in composites.

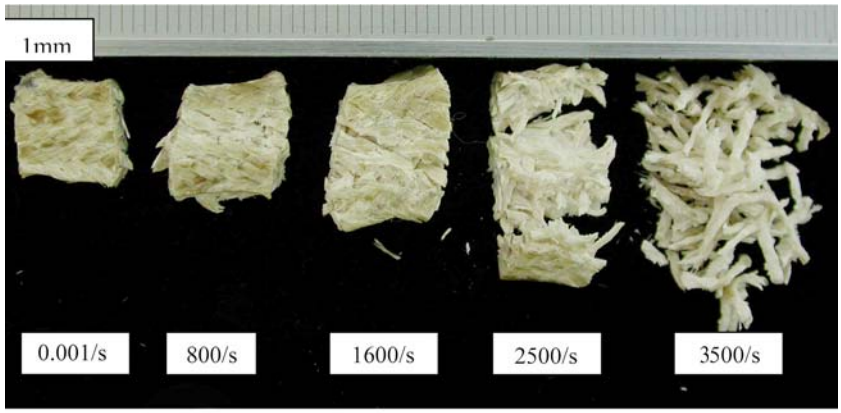

(a) out-of-plane direction

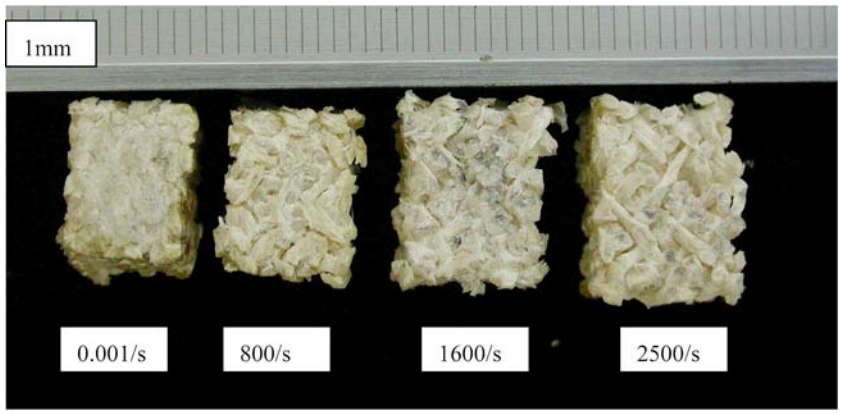

(b) in-plane direction

Fig. 10 Compressive failure of 3D braided composites in the out-of-plane and in-plane directions at various strain rates

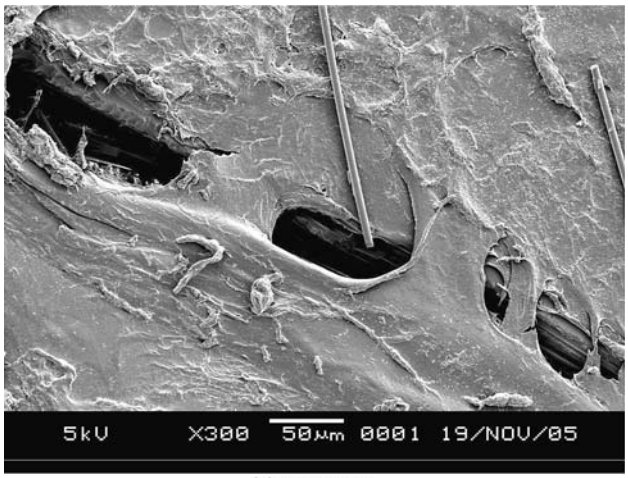

(a) Quasi-static

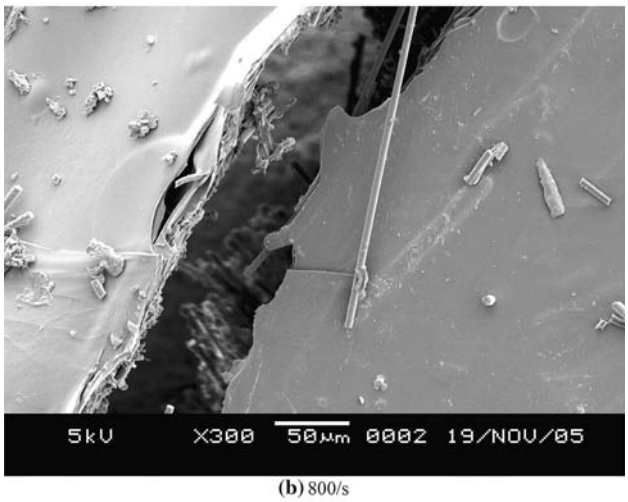

(b) 800/s

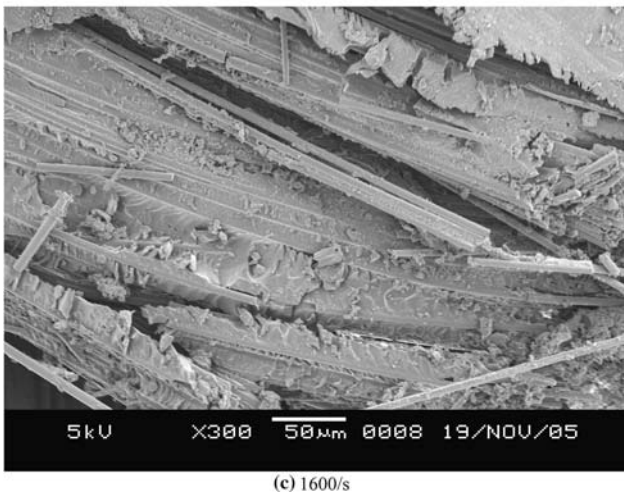

(c) 1600/s

Fig. 11 Microscopic damage of composites at different strain rates under out-of-plane compression

This manifests the shear failure between two braided tows under higher stress than the matrix strength. As the strain increases, the braided tows breakage accompanied with the shear (sliding evidence in Fig. 11(c)) occur. When the strain rate is greater than 2,500/s, the whole composite coupon became into debris because of the difference of stress wave velocity between tows and matrix, and also the higher energy rate applied to composite coupons.

Figure 10(b) presents the failure mode of the materials in the in-plane direction. No shear failure or other failure modes can be found in Fig. 10(b). As the strain rate increases, only larger compressive deformation can be observed. Furthermore, the cross-sections of the material coupons after compressive testing keep the same rectangular shape as considering before testing because of their quasi-isotropic structure. Considering the failure photographs with the stress–strain curves, it could be found that matrix cracking is the main failure mechanism for in-plane compression (Fig. 12(a) and (b)). When stress runs up to maximum value, the cracks in matrix of the composite will propagate. Only the braided preform bears the in-plane impulsive loading (Fig.12(c)). This resulted in a linear increase of stress in the specimen until the matrix was cracked and then only 3D braided preform bore the impulsive load. Stress decreases from the peak value only when the 3D braided preform bore the load.

From Fig. 10(a) and (b), it was found that the failure modes for out-of-plane and in-plane loading are completely different. The failure mode under out-of-plane loading is shear failure for strain rates of 0.001/s to 3,500/s, while that for in-plane loading is cracking of the matrix from strain rates of 0.001/s to 2,500/s.

Conclusions

The 4-step 3D braided composites exhibit strain rate sensitivity during compression loading in out-of-plane and in-plane directions. In quasi-static loading, the compressive stiffness is higher in the out-of-plane direction than in the in-plane direction. For high strain rate compression, the compressive stiffness for in-plane loading is higher than that for out-of-plane loading at same strain rate. The compressive stiffness is more sensitive to strain rate in the in-plane direction. The composites have higher compression strength in the out-of-plane direction than in the in-plane direction. The failure stress of the composites occurs at nearly the same sensitive to strain rate in the two compression directions. The failure strain decreases with the increase of strain rate. Failure strains at high strain rate are drastically decreased when compared with quasi-static compression. The photographs of the

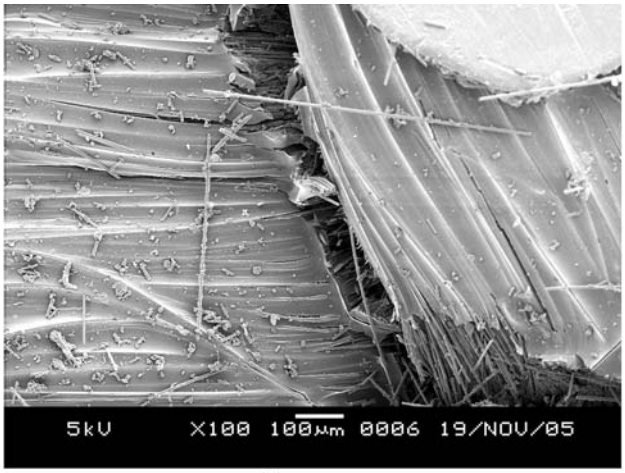

(a) Quasi-static

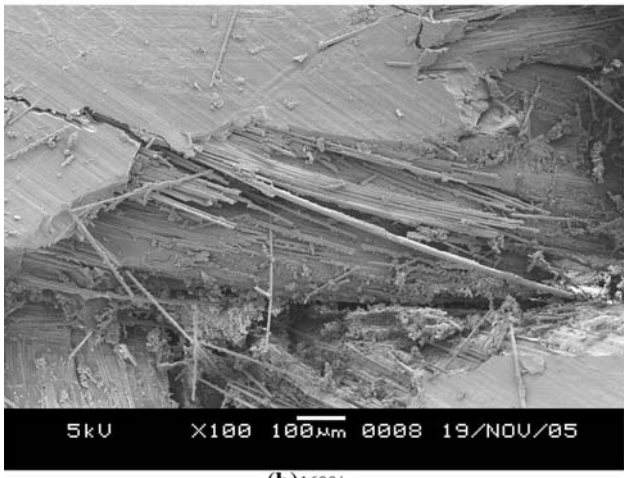

(b) 1600/s

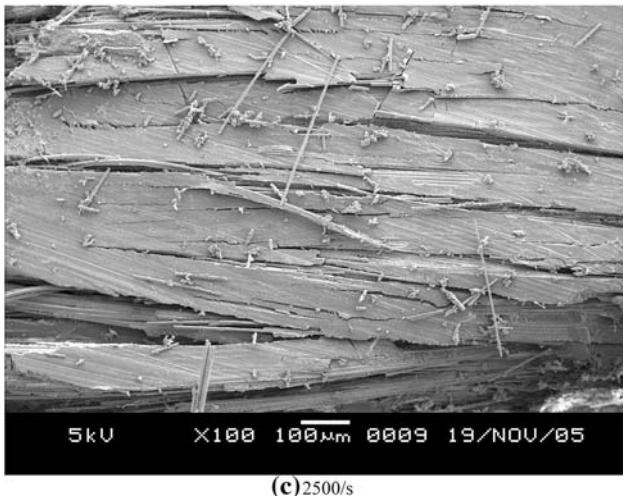

(c) 2500/s

Fig. 12 Microscopic damage of composites at different strain rates under in-plane compression

damaged composites at various strain rates in the out-of-plane and in-plane directions show that the damage mode is completely different for the two directions. The shear failure is the main mode in out-of-plane compression. Matrix cracking is the main failure mode for in-plane compression.

Acknowledgements The authors of this paper gratefully acknowledge the supports of the Chinese National Science Foundation (NSFC 19902016) and the Natural Science Foundation of Shanghai Municipality (04ZR14009). The author of Bohong Gu, also acknowledges the helps from Mr. Alexi Rakow, Ph.D. Candidate of Structures and Composites Laboratory, Stanford University for revising English of the paper when the author is a visiting scholar at this laboratory. Furthermore, authors gratefully appreciate the constructive opinions of anonymous reviewers which lead to the further analysis of compression damage mechanism under different strain rates.

References

1. Hosur MV, Alexander J, Vaidy UK, Jeelani S (2001) Compos Struct 52:405
2. Haque A, Hossain MK (2003) J Composite Mater 37:627
3. Hosur MV, Alexander J, Vaidya UK, Jeelani S, Mayer A (2004) Compos Struct 63:75
4. Hosur MV, Abraham A, Jeelani S, Kvaidya U (2001) J Composite Mater 35:1111
5. Hosur MV, Adya M, Vaidya UK, Mayer A, Jeelani S (2003) Compos Struct 59:507
6. Sun BZ, Gu BH, Ding X (2005) Polym Test 24:447
7. Sun BZ, Yang L, Gu BH (2005) AIAA J 43:994
8. Chou TW (1992) Microstructural design of fiber composites. Cambridge University Press, Cambridge
9. Meyers MC (1995) Dynamic behavior of materials. John Wiley & Sons, New York